ACOUSTICS 2017 PERTH
SOUND, SCIENCE AND SOCIETY

Sound radiation from the open end of pipes and ducts in the presence of mean flow

Ray Kirby (1), Wenbo Duan (2)

(1) Centre for Audio, Acoustics and Vibration, University of Technology Sydney, Sydney, Australia
(2) Brunel Innovation Centre, Brunel University London, London, United Kingdom

ABSTRACT

The radiation of sound from the open end of pipes and ducts is a common problem in environmental noise control. Examples include radiation from ductwork in heating, ventilation and air-conditioning systems, noise emissions from exhaust stacks in industrial power plants, as well as radiation from turbofan engines. These open duct terminations represent a relatively simple mechanical structure; however, the acoustics is significantly more complicated and this is especially true when a mean gas flow is present. This article presents an efficient numerical model suitable for analysing sound radiation from an unflanged duct termination, and introduces a method for including a uniform mean fluid flow in the exterior region away from the termination. An example of sound radiation from a turbofan engine is then investigated.

1 INTRODUCTION

Many applications in acoustics involve the propagation of sound in pipes or ductwork. The sound source is normally a fluid moving device such as a fan or power generator and this moving fluid is almost always expelled to the atmosphere through an open duct termination. This facilitates the easy removal of the fluid, however the open end also impacts on the acoustics of the duct system because the change in impedance at the termination both reflects and scatters an incident sound wave. Therefore, open duct terminations can significantly impact on the acoustics of a system and they should be included in the calculation of system performance. Furthermore, the role they play in scattering sound is also important when measuring noise radiation and meeting environmental noise regulations. Accordingly, this article examines the problem of noise radiation from open duct terminations and discusses a numerical approach to calculating sound reflection and scattering. The article also develops a method for adding a uniform mean fluid flow in the region outside of the duct termination.

Common examples of open duct terminations include the exhaust and intake systems for power generation, such as gas turbines and turbofans used in aircraft, as well as internal combustion engines. Other examples include heating ventilation and air-conditioning (HVAC) systems. The noise emitted by these applications is normally quantified using a multiple number of measurements undertaken in the surrounding environment. These measurements must account for the directionality of the sound pressure field, and this is linked to the noise source as well as the scattering effect of the open termination. Accordingly, understanding the way in which sound radiates from terminations is important in achieving an optimised acoustic design for a system. The radiation of sound from open ended duct terminations presents a classical problem first studied by Rayleigh that appears, at least at first glance, to be reasonably straightforward. However, in reality open ended terminations are a complex problem and they do not lend themselves to straightforward analytic methods. For example, the most well-known analytic work on the subject is by Levine and Schwinger (1948), who relied on a Wiener-Hopf approach to study an unflanged duct. Alternative methods normally rely on some form of numerical discretisation and this requires one to enforce the Sommerfeld radiation condition at infinity. This is readily achieved using the boundary element method (BEM), and Dalmont et al. (2001) used boundary elements to examine sound radiation from a finite length unflanged duct. Burnett (1994) investigated an alternative approach using infinite elements to discretize the outer region, and then compared the computational time of this method with the BEM. Burnett reported that the infinite element method is two or three orders of magnitude faster than the BEM for the same accuracy. However, infinite elements cannot be placed close to regions of high modal scattering and so it is often necessary to place them a long way from the outlet of a duct termination, especially at higher frequencies. This makes infinite elements less attractive for larger problems and higher frequencies. The BEM also becomes less efficient when regions of internal non-uniformity are present, which is the case when non-uniform fluid flow is present in a duct system. Therefore it is common to focus on the use of finite element based methods when studying radiation from open ducts, especially when mean flow is present, see for example the study of turbofan engines by Astley et al (2011). The finite element method does, however, present the problem of enforcing the Sommerfeld radiation boundary condition. To address this, one may use infinite elements, even when mean flow is present, see Eversman (1999), or the DtN method which applies the boundary conditions locally on an artificial surface surrounding the outlet of the pipe

Givoli (2004). Perfectly matched layers (PML) can also be used in the outer domain, as these damp down outwards going waves; however, PMLs are computationally expensive as one needs to mesh a large outer domain, especially at higher frequencies.

This article introduces an alternative numerical method developed by the authors for analysing sound radiation from open ended duct terminations, see Duan and Kirby (2012). It is shown in this article that this method may be extended to include the effects of mean fluid flow, so that it is applicable to a wider range of noise control problems. Moreover, the method has the advantage of working over a wide frequency range and it can accommodate geometries with an arbitrary cross-section, so that it can readily be applied to rectangular as well as circular geometries. The method is also sufficiently general to be used in the study of complex duct terminations, such as those found in HVAC systems, although this type of problem will not be discussed here. Instead, the article will focus on introducing mean flow into a model for sound radiation from a turbofan engine. This example problem is chosen because it provides a relatively straightforward flow field in the regions away from the end of the pipe.

2 THEORY

The numerical method presented here is based on a hybrid modal-finite element approach. The basic principles behind this hybrid approach were discussed by Kirby (2008), and it is flexible enough to be used in many different applications in guided waves, see for example Kirby et al. (2013) and Duan et al. (2016). The method relies on the use of modal solutions for uniform regions, and a full finite element discretisation for non-uniform regions. Thus, for uniform regions the acoustic pressure is expanded as an infinite set of eigenmodes and, crucially, expansions can be obtained for exterior regions using Hankel functions for a two-dimensional problem, and spherical Hankel functions for a three-dimensional problem. Moreover, this approach has the advantage of automatically satisfying the Sommerfeld radiation condition because the sound pressure in the exterior region is written as a set of outward propagating modes and the amplitudes of the reflected modes are set equal to zero. However, the use of Hankel basis functions normally relies on a regular geometry such as a circle (two dimensions), or a sphere (three dimensions). Of course, regular geometries do not appear for an open end, see for example the truncated circle in Figure 1. Thus, the key challenge when applying a hybrid approach to open ended ducts is obtaining a modal basis for the exterior scattering problem. It was shown by Duan and Kirby (2012) that this can be accomplished provided the sound field in the exterior region is separable, and this method is reviewed here first for zero mean flow, and then the addition of flow is discussed in the section that follows.

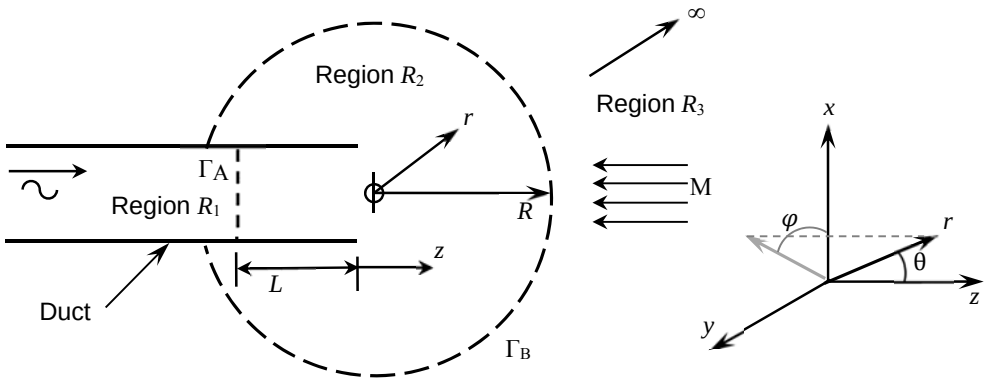

Figure 1: Geometry of problem, with sound incident in the position z direction region 1, and a mean flow Mach number M in the negative z direction.

2.1 No mean flow

In the absence of mean flow, the governing wave equation for region q ($q = 1,2,\text{or } 3$), is given as

$$\nabla^2 p'_q - \frac{1}{c_0^2}\frac{\partial^2 p'_q}{\partial t^2} = 0, \tag{1}$$

where p' is pressure, t is time, and c_0 is the speed of sound in the fluid. For the uniform duct, the pressure is expanded over an infinite set of eigenmodes, to give

$$p'_1(r,\theta,z;t) = \sum_{m=0}^{\infty}\sum_{n=0}^{\infty} \mathrm{F}_{m,n}\Phi_{m,n}(r)e^{i(\omega t - n\theta - k_0\lambda_m z)} + \sum_{m=0}^{\infty}\sum_{n=0}^{\infty} \mathrm{A}_{m,n}\Phi_{m,n}(r)e^{i(\omega t - n\theta + k_0\lambda_m z)}. \quad (2)$$

Here, r,θ,z form a cylindrical co-ordinate system, t is time, ω is the radian frequency, $k_0 = \omega/c_0$ and $i = \sqrt{-1}$. In addition, for mode (m,n), $\Phi(r)$ is the eigenvector and λ the eigenvalue, with $\mathrm{F}_{m,n}$ and $\mathrm{A}_{m,n}$ modal amplitudes.

The key challenge for region 3 is obtaining an eigenexpansion for a truncated circle in two dimensions, or a truncated sphere, or cone, in three dimensions. To achieve this, the sound pressure in region 3 is written as

$$p'_3(r,\theta,\varphi;t) = \sum_{m=0}^{\infty} \mathrm{B}_m \Upsilon_m(r)\Psi_m(\theta,\varphi)e^{i\omega t}. \quad (3)$$

Here, r,θ,φ form a spherical co-ordinate system in region R_3, and B_m is the modal amplitude. The sound pressure field is separated into a radial component Υ_m and a transverse component $\Psi(\theta,\varphi)$. This separation is crucial to writing the outer sound pressure field as a series of outgoing modes, which then allows the exact implementation of the Sommerfeld radiation condition (by setting the modal amplitude for inward travelling waves equal to zero). Substituting Eq. (3) into the governing wave equation, and separating variables yields

$$\Upsilon_m(r) = h^{(2)}_{\sigma_m}(k_0 r), \quad (4)$$

where $s_m^2 = \sigma_m(\sigma_m + 1)$ and

$$\nabla^2_{\theta\varphi}\Psi(\theta,\varphi) + s^2\Psi(\theta,\varphi) = 0. \quad (5)$$

Thus, one first solves the eigenproblem in Eq. (5) to find s and then the radial displacement is found from Eq. (4), where $h^{(2)}_{\sigma_m}$ is a spherical Hankel function of the second kind, of order σ_m. Equation (5) is an eigenproblem over the outer surface of region R_2, which is a one dimensional problem for a circle, and a two dimensional problem for a cone, which is not difficult to solve and does not take up too much computer memory. Following the solution of the respective eigenproblems in regions R_1 and R_3, the only unknown variables in Eqs. (2) and (3) are the modal amplitudes. These are obtained following the solution of the scattering problem, and this requires the modal solutions to be joined to the finite element discretization in region R_2. This is implemented by enforcing continuity of pressure and normal velocity over the interface between each region Γ_A and Γ_B. This process is described in detail in the article by Duan and Kirby (2012), and following this one obtains a linear system of equations that can be solved to find the unknown modal amplitudes and the acoustic pressure. To quantify the influence of the open end, an energy balance is carried out and the transmission loss (TL) is defined as the ratio of the incident to transmitted sound power, which gives

$$\mathrm{TL} = -10\log_{10}\left[\frac{1}{k_0^2}\frac{\sum_{m=0}^{M_{tr}} \mathrm{H}_m|B_m|^2}{\sum_{m=0}^{M_{inc}} \lambda_m \mathrm{I}_m|F_m|^2}\right] \quad (6)$$

where, M_{inc} and M_{tr} denote the number of cut-on modes for the incident and transmitted waves, respectively; and $\mathrm{I}_m = \int |\Phi_m(r,\theta)|^2\, d\Gamma_A$ and $\mathrm{H}_m = \int |\Psi_m(\theta,\varphi)|^2\, d\Gamma_B$.

2.2 Addition of Mean flow

The presence of a mean gas flow is common in most applications. However, the addition of flow into this numerical model is not straightforward and so only a simple mean flow profile is considered in this study. This assumes a mean flow of velocity v_z is incident normal to the plane of the pipe, so that it is parallel to the z axis and in a direction from right to left, see Fig. 1. That is, the mean flow velocity is defined at $z = +\infty$ as $\mathbf{v} = [0,0,-\mathrm{v}_z]$, with a Mach number $M_z = \mathrm{v}_z/c_0$ is defined in the outer region. This flow then impinges upon the duct, with some flow going into the duct, and some flow around the duct. This type of velocity profile is seen in turbofan applications, see for example Eversman (1999). Furthermore, it is necessary for the velocity profile to be uniform in the outer region so that the acoustic variables remain separable and one may then expand the pressure as a set of propagating eigenmodes in the same way as before. Of course, the use of the finite element discretisation in region 2 is designed to allow for more complex flow patterns and so it is assumed that any complex flow patterns are restricted to this region only. Furthermore, the static potential flow field is calculated independently of the acoustic field, so that the mean flow velocity field is obtained first, and this is then substituted into the acoustic wave equation to solve for the acoustic pressures. To obtain the flow field, only a simplified potential flow solution is used here as the focus remains on obtaining the acoustic solution. Accordingly, in the discussion that follows, it is assumed that the potential velocity field has been solved first, and the values obtained are then added into the acoustic equations. The governing wave equation when flow is present is then given by Pierce (1990):

$$\nabla \cdot (\rho_0 \nabla \phi) - \rho_0 \left(\frac{\partial}{\partial t} + \mathbf{v} \cdot \nabla\right) \frac{1}{c_0^2} \left(\frac{\partial}{\partial t} + \mathbf{v} \cdot \nabla\right) \phi = 0. \quad (7)$$

Here, ρ_0 is the density of the fluid, and ϕ is a velocity potential defined as $\phi = -\rho_0(\partial/\partial t + \mathbf{v} \cdot \nabla)\phi$. To implement the hybrid method in the same way as for the no flow case, it is necessary to obtain a separable solution to the governing wave equation in region R_3. To accomplish this, a Lorenz transformation is used, and assuming a uniform flow in region R_3, with $\beta = \sqrt{1 - M_z^2}$, this gives

$$X = x/\beta,\ K = k/\beta, \text{ and } T = \beta t + M_z X/c_0. \quad (8)$$

This delivers a revised modal expansion for region R_3 of the form,

$$\phi_3(r, \theta, \varphi) = \psi_3(R, \Theta, \varphi) e^{iKM_z R\cos\Theta}. \quad (9)$$

where $\tan\Theta = \beta\tan\theta$ and $\beta R = r\sqrt{1 - M_z^2 \sin^2\theta}$. This shift in co-ordinates then allows the governing equation in the outer region to be written as

$$\nabla^2 \psi_3 + K^2 \psi_3 = 0 \quad (10)$$

which delivers a (separable) Helmholtz Equation for region R_3. Following the approach in the previous section, this may be solved using an expansion for ψ_3 of the form

$$\psi_3(R, \Theta, \varphi) = \sum_{m=0}^{\infty} B_m h_{\tilde{\sigma}_m}^{(2)}(KR) \vartheta_m(\Theta, \varphi). \quad (11)$$

The values of $\tilde{\sigma}_m$ and ϑ_m are then found in the same way as before, but this time in the shifted co-ordinates. Following this, the modal amplitudes and velocity potential is found in each region using a finite element mesh in region R_2, and the usual modal expansion (with flow) in region R_1.

3 RESULTS AND DISCUSSION

The radiation problem is solved here for a pipe of circular cross-section, which after taking advantage of symmetry enables a solution to be obtained in two dimensions only. This is achieved by separating the sound field in region 3 into two components, so that as $\Psi_m(\theta, \varphi) = \widetilde{\Psi}_m(\varphi) e^{-in\theta}$, where the angular dependence in the θ direction maps onto the eigenexpansion chosen in region 1. This then enables a two dimensional discretisation of the problem in region 2 and a one dimensional discretisation over Γ_A and Γ_B. In the examples presented here, quadratic line, triangular and rectangular elements are used. Following solution of the problem, post-processing enables the sound pressure field to be obtained for the entire region, and in Fig. 2 this is illustrated for an example problem with a planar incident sound field ($F_{0,0} = 1,\ F_{m,n} = 0$, for $m > 0$ and $n > 0$). Here, the radius of the inlet duct is 0.05 m, and the sound pressure distribution is shown at 400 Hz with $c_0 = 343.2244$ m/s.

Figure 2 plots absolute value of the sound pressure $|p|$, and the boundary Γ_B is shown on the diagram as a white dashed line. This figure clearly shows that high levels of energy are reflected back into the duct, which causes a strong standing wave to form in the duct and a relatively quick drop in the sound pressure level away from the open end. It is also noticeable that the sound transmitted away from the open end is close to planar at about two to three times the duct radius.

In Fig. 3 the excitation frequency is increased to 4 kHz, although a plane wave incident sound field is maintained. It is clear that when the frequency is increased above that of the first cut-on mode in region 1, the energy in the duct largely escapes from the open end. This lowers the sound transmission loss of the open end, and the energy is seen to “beam” out of the duct and deliver relatively high sound pressure levels directly in front of the open end. However, it is also seen that high pressure is localised close to the pipe exit and this effect may potentially be important in the design of treatments for noise from open ends, for example those used in HVAC systems. Figure 3 also shows that for plane wave excitation a shadow zone is still present when one moves in the transverse direction away from the duct exit plane. This delivers a highly directional sound field. Figure 3 is also helpful in illustrating the seamless continuity that can be obtained in the sound pressure field, so that if one removes the white dashed line from Fig. 3 it would not be possible to identify the join between the finite element region and the outer modal expansion.

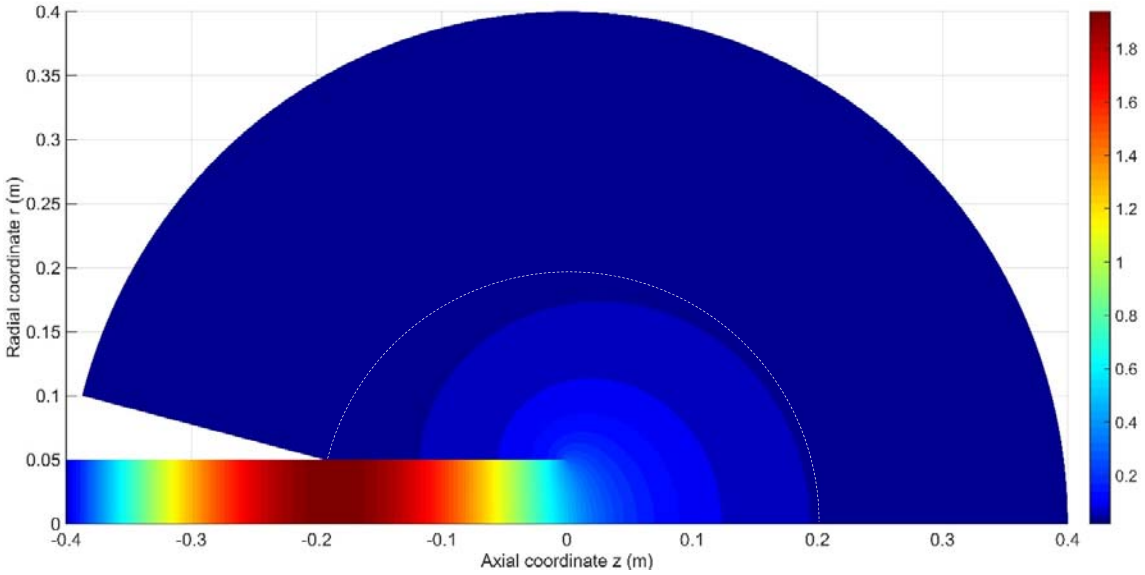

Figure 2: No flow. Magnitude of acoustic pressure $|p|$ for plane wave excitation in circular duct at 400 Hz.

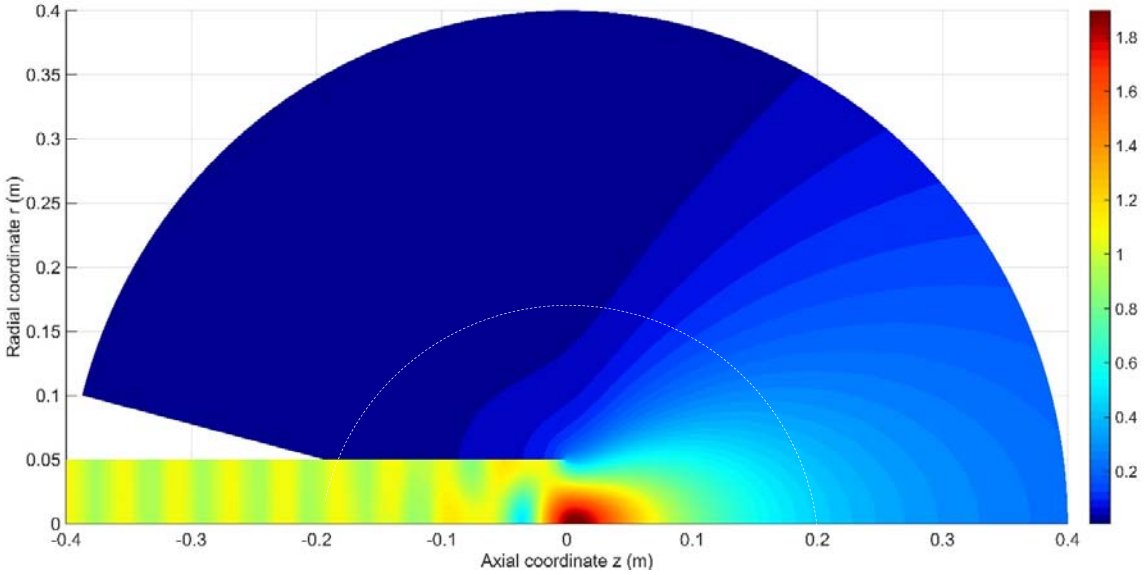

Figure 3: No flow. Magnitude of acoustic pressure $|p|$ for plane wave excitation in circular duct at 4 kHz.

Figures 2 and 3 illustrate the influence of frequency on the transmission of sound through the open end of a duct. This can be quantified in the form the transmission loss TL, which is defined in Eq. (6). Duan and Kirby (2012) report the following expressions obtained using this approach: for an unflanged circular duct

$$\mathrm{TL} = 10\log_{10}\left[1 + \frac{1}{(k_0 a)^2}\right]. \tag{12}$$

where a is the duct radius. And for an unflanged rectangular duct

$$\mathrm{TL} = 10\log_{10}\left[1 + \frac{0.3909H}{(k_0 a)^2}\right], \tag{13}$$

where the rectangular duct has dimensions $2a \times 2b$ and $H = a/b$ with $H \geq 1$.

The TL values reported above, and the sound pressure plots reported so far, rely on a planar incident sound field. However, in practice it is common to encounter multi-modal excitation, and it is well known that turbomachinery generates tonal as well as broad-band noise. It is, therefore, interesting to investigate the behaviour of higher order incident modes, and these are chosen here to be circumferential modes, so that $m = 0$ and $n > 0$. Accordingly, in Figure 4, the sound pressure distribution for the mode (0,2) is shown, and here one can see that the energy in the duct is now concentrated towards the outer wall, and this is refracted by the pipe termination. This leads to higher sound pressure levels being found at larger angles to the centreline, as well as in the shadow region of the duct.

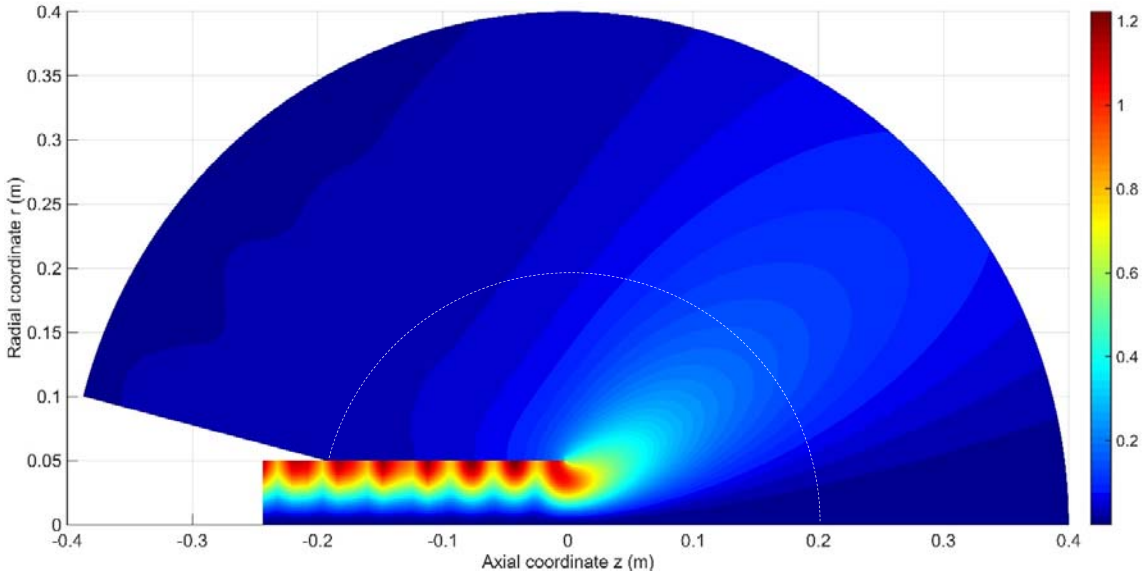

Figure 4: No flow. Magnitude of acoustic pressure $|p|$ for multi modal excitation ($n = 2$) in circular duct at 6 kHz.

The sound pressure field seen in Figure 4 generates a more complex directivity pattern, and this is shown in Fig. 5 where the pressure pattern is compared at an outer radius of 0.2 m (the dashed white line) for the two planar excitations in Figs. 2 and 3, and the higher order mode in Fig. 4.

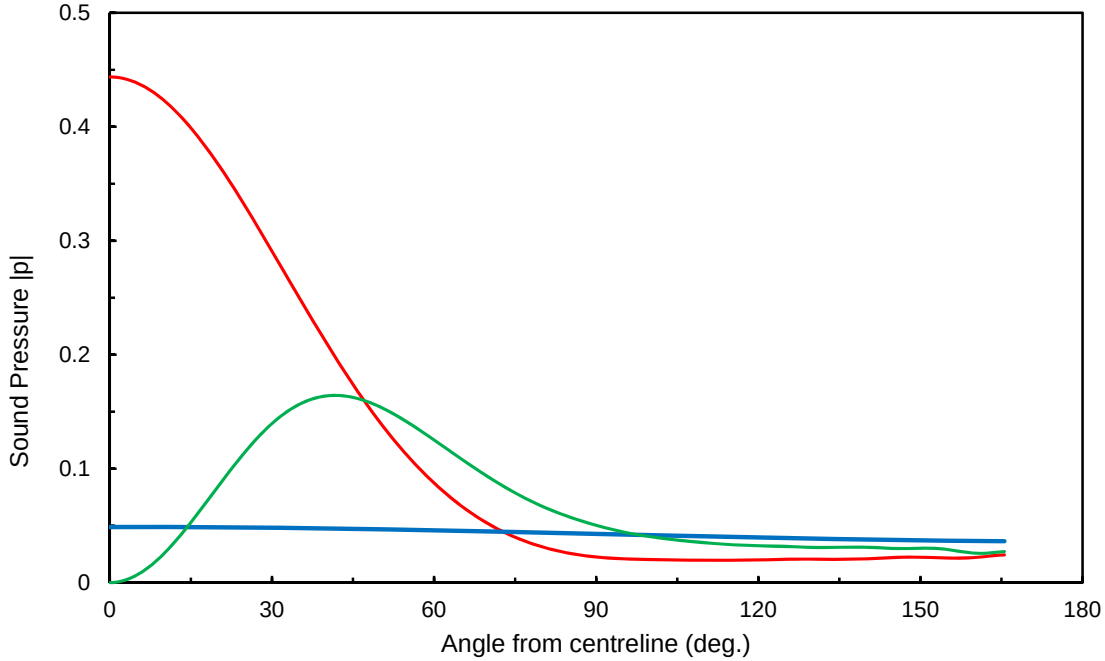

Figure 5: No flow. Magnitude of acoustic pressure $|p|$ for a circular duct at $r = 0.2$ m.
, 400 Hz, $n = 0$; , 4 kHz, $n = 0$; , 6 kHz, $n = 2$

One can see in Fig. 5 that at 400 Hz the relative radiated sound pressure level is low, as energy is reflected back by the pipe duct end, whereas at higher frequencies energy is permitted to escape from the duct. Moreover, Fig. 5 illustrates the potential complexity of the pressure patterns for an open-ended duct, and if energy is propagating in a number of incident eigenmodes then these patterns can combine to produce more complex distributions at higher frequencies, although the exact way in which these patterns combine will depend on the sound source. The behaviour illustrated in Fig. 4 is particularly relevant to turbines and those turbofan engines found in aircraft. This is because these applications have large numbers of blades and this can transfer energy into very higher order circumferential, or spinning, modes. This behaviour can be seen by increasing the frequency (relative to the duct radius), and here the frequency is increased to 12 kHz so that one drives the mode $m = 0 \text{ and } n = 9$. The resulting sound pressure field is shown in Fig. 6 and here one can see that sound radiates at an even higher angle to the centreline than seen previously. Moreover, some energy is trapped in the duct, even at these high frequencies, although significant levels of energy are still likely to escape.

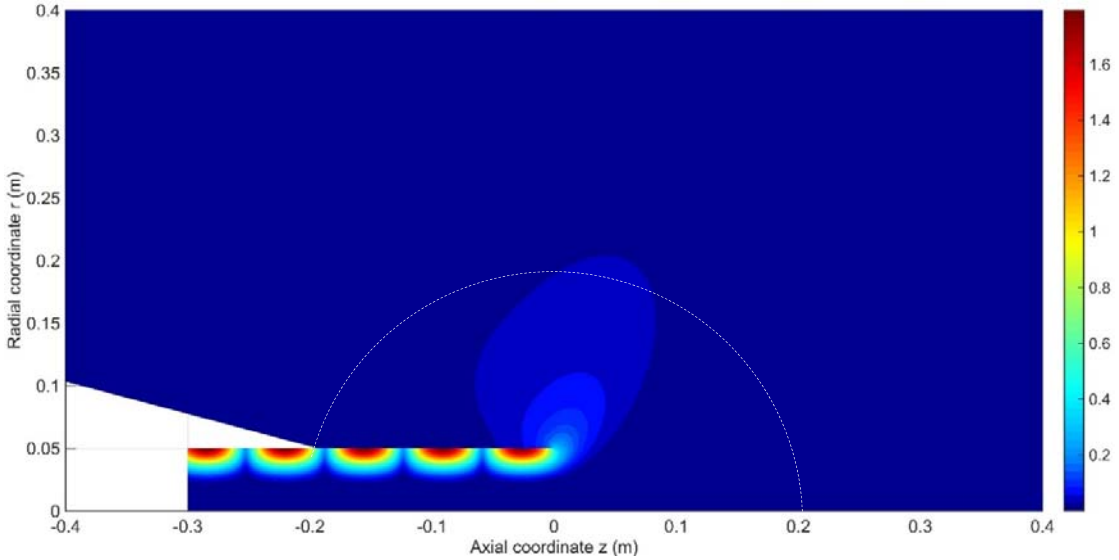

Figure 6: No mean flow. Magnitude of acoustic pressure $|p|$ for excitation of single higher order mode ($n = 9$) in circular duct at 12 kHz.

In Fig. 7, the effect of mean flow is added to the problem studied in Fig. 6. The mean flow has a Mach number of $M_z = 0.3$ incident on the duct in the negative z direction. It can be seen that the mean flow changes the directivity pattern, so that the magnitude of the sound pressure increases outside of the pipe. This effect is shown in more detail in Fig. 8, where the pressure patterns are compared with and without flow at an outer radius of 0.2 m.

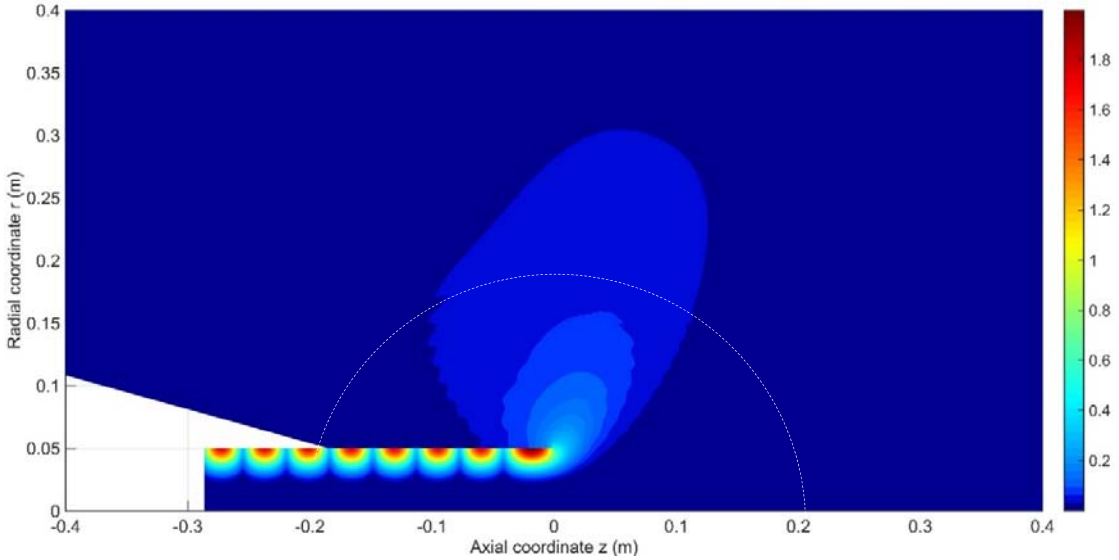

Figure 7: Mean flow $M_z = 0.3$. Magnitude of acoustic pressure $|p|$ for excitation of single higher order mode ($n = 9$) in circular duct at 12 kHz.

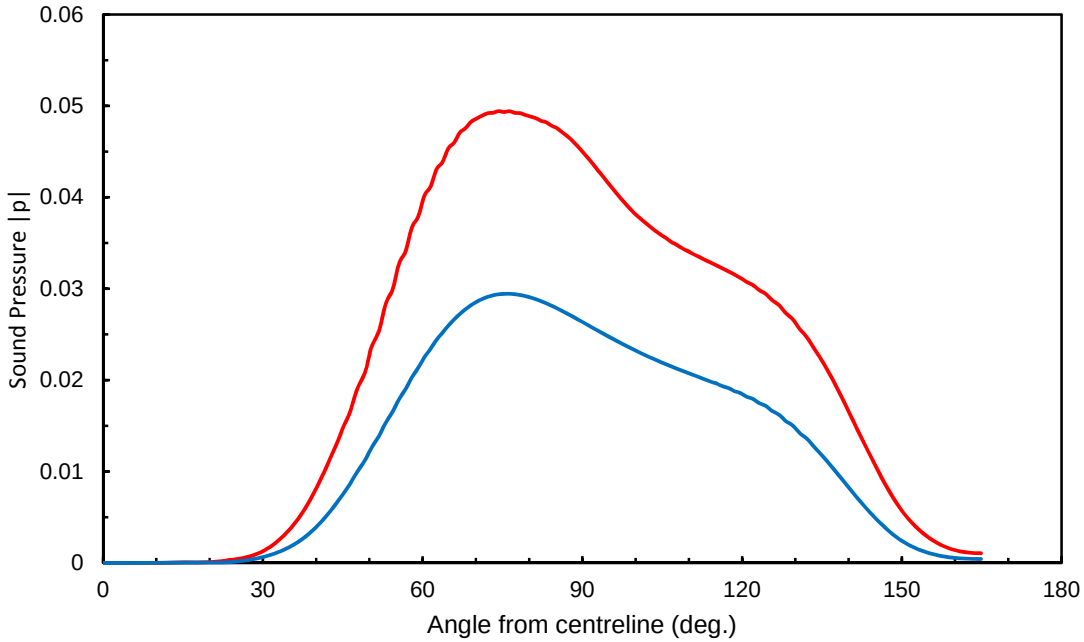

Figure 8: Magnitude of acoustic pressure for excitation of single higher order mode ($n = 9$) in circular duct at 12 kHz. ——— , $M_z = 0$, ——— , $M_z = 0.3$

Finally, it is interesting to compare the results obtained with flow against those previously reported in the literature by Eversman (1999), who used infinite elements in the outer region. In order to facilitate this comparison for a pipe radius of 50 mm, it is necessary to scale the frequency up to 27.4 kHz to provide the same conditions as those used by Eversman [for a bigger duct]. It can be seen in Fig. 9 that behaviour is observed that is similar to that seen in the previously when $n > 0$. This pressure profile is also seen to compare reasonably well with the plots presented by Eversman. Furthermore, this sound pressure field serves to illustrate the complexity of the problem and the challenge associated with accurately predicting and measuring the sound pressure distribution from the open end of a duct or pipe.

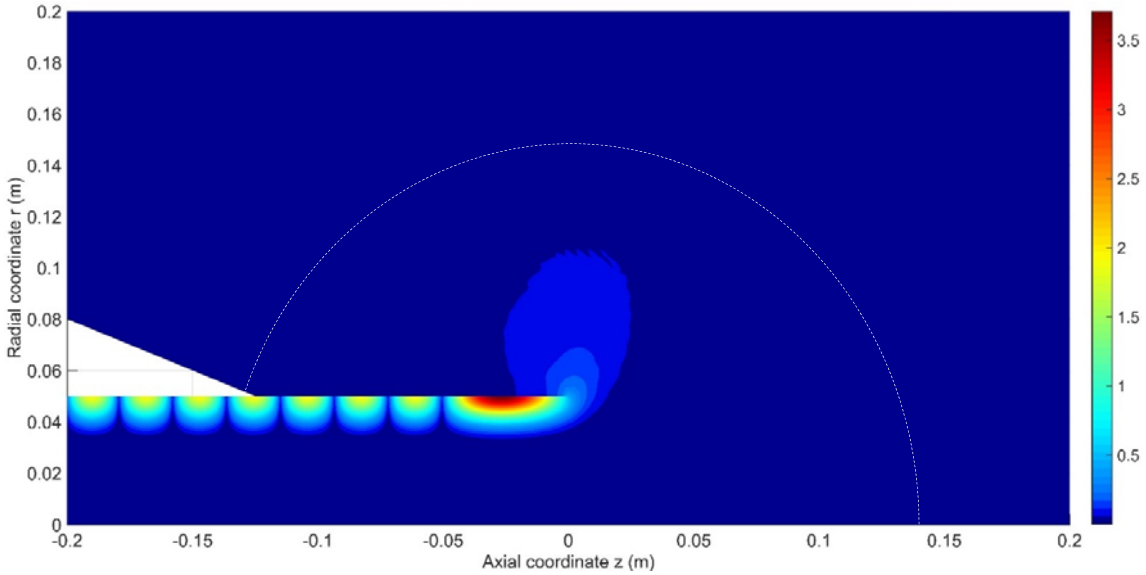

Figure 9: Mean flow $M_z = 0.3$. Magnitude of acoustic pressure $|p|$ for excitation of single higher order mode ($n = 23$) in circular duct at 27.4 kHz.

4 CONCLUSIONS

This article presents a numerical method for obtaining the acoustic behaviour of an open ended duct or pipe. The numerical method makes use of a modal expansion in the region exterior to the duct in order to enforce exactly the Sommerfeld radiation condition. This then facilitates the introduction of a numerically efficient approach to solving the problem as one only needs to solve an eigenproblem over the outer surface of the finite element domain. It is also shown that this method may be extended to include mean fluid flow, but only if the flow in the outer region is uniform. This enables a Lorenz transformation to be used that then restores a separable equation in the outer region. Following this, the problem with flow may be solved in the same was as that described for zero mean flow.

Predictions for plane wave and higher order modal excitation are presented here. It is seen that the pressure patterns generated by scattering from the open end of the pipe become very complex. This is especially true when higher order modes are excited in the pipe. Accordingly, for complex noise sources, such as those found in turbomachinery, it is likely that the radiated sound pressure field will be complex and susceptible to small changes in local conditions, including the presence of mean fluid flow. For example, this may be important when measuring directivity patters in the presence of wind. The influence of the open end of a pipe is also quantified using a sound power balance, and two relatively simple equations are repeated here for the TL of the open end of a circular and rectangular duct in the absence of mean flow. Further work is required to quantify the effect of the mean flow on these values for TL, including the effect of changes in mean flow speed and direction. This will then enable environmental conditions to be factored into calculations on the acoustics of open-ended terminations.

REFERENCES

Astley, R.J., Sugimoto, R., Mustafi P. 2011. 'Computational aero-acoustics for fan duct propagation and radiation. Current status and application to turbofan liner optimisation.' *Journal of Sound and Vibration* 330: 3832-3845.
Burnett, D.S. 1994. 'A three-dimensional acoustic infinite element based on a prolate spheroidal multipole expansion." *Journal of the Acoustical Society of America*, 96: 2798-2816.
Dalmont, J.P., Nederveen, C.J., & Joly, N. 2011. 'Radiation impedance of tubes with different flanges: Numerical and experimental investigations,' *Journal of Sound and Vibration*, 244: 505-534.
Duan, W., & Kirby, R. 2012. 'A hybrid finite element approach to modeling sound radiation from circular and rectangular ducts'. *Journal of the Acoustical Society of America*, 131: 3638-3649.
Duan, W., Kirby, R., & Mudge, P. 2016. 'On the scattering of elastic waves from a non-axisymmetric defect in a coated pipe.' *Ultrasonics 65*: 228-241.
Eversman, W. 1999. 'Mapped infinite wave envelope elements of acoustic radiation in a uniformly moving medium,' *Journal of Sound and Vibration* 224: 665-687.
Givoli, D. 2004. 'High-order local non-reflecting boundary conditions: A review.' Wave Motion. 39, 319-326.
Kirby, R. 2008. 'Modeling sound propagation in acoustic waveguides using a hybrid numerical method'. *Journal of the Acoustical Society of America* 124: 1930-1940.
Kirby, R., Zlatev, Z., & Mudge, P. 2013. 'On the scattering of longitudinal elastic waves from axisymmetric defects in coated pipes'. *Journal of Sound and Vibration* 332: 5040-5058.
Levine, H., Schwinger, J. 1948. "On the radiation of sound from an unflanged circular pipe," Phys. Rev. 73: 383-406.
Pierce, A.D. 1990. 'Wave equation for sound in fluids with unsteady inhomogeneous flow.' *Journal of the Acoustical Society of America* 87: 2292-2299.
Rayleigh Lord. 1945. '*The theory of Sound*'. Dover, New York, vol. II, chapter 16.